Iterative backflow renormalization procedure for many-body ground-state wave functions of strongly interacting normal Fermi liquids

Michele Taddei,[1] Michele Ruggeri,[2] Saverio Moroni,[2] and Markus Holzmann[3,4,5]

[1]*Dipartimento di Fisica, Sapienza Università di Roma, Piazzale A. Moro 2, I-00185 Roma, Italy*

[2]*DEMOCRITOS National Simulation Center, Istituto Officina dei Materiali del CNR and SISSA, Via Bonomea 265, I-34136 Trieste, Italy*

[3]*LPTMC, UMR 7600 of CNRS, Université Pierre et Marie Curie, Paris, France*

[4]*LPMMC, UMR 5493 of CNRS, Université Grenoble Alpes, F-38100 Grenoble, France*

[5]*Institut Laue Langevin, BP 156, F-38042 Grenoble Cedex 9, France*

(Received 9 January 2015; revised manuscript received 5 February 2015; published 2 March 2015)

We show how a ground-state trial wave function of a Fermi liquid can be systematically improved by introducing a sequence of renormalized coordinates through an iterative backflow transformation. We apply this scheme to calculate the ground-state energy of liquid ^{3}He in two dimensions at freezing density using variational and fixed-node diffusion Monte Carlo. Compared with exact transient estimate results for systems with a small number of particles, we find that variance extrapolations provide accurate results for the true ground state together with stringent lower bounds. For larger systems these bounds can in turn be used to quantify the systematic bias of fixed-node calculations. These wave functions are size consistent and the scaling of their computational complexity with the number of particles is the same as for standard backflow wave functions.

DOI: 10.1103/PhysRevB.91.115106 PACS number(s): 67.30.E−, 02.70.Ss

I. INTRODUCTION

To overcome the fermion-sign problem, many fermion quantum Monte Carlo (QMC) calculations rely on the fixed-node (FN) approximation where the nodes of a trial wave function, ψ_T, are imposed as a boundary condition on the many-body Schrödinger equation, which can then be solved by projector Monte Carlo methods [1]. Since the nodal surfaces of the exact ground-state wave function are in general unknown, the energies of FN calculations do not converge to the exact ground-state energy but remain above it by an unknown amount. Although methods which do not rely on the FN approximation have been developed [2–6], they are in general limited to small systems, as their computational cost grows exponentially with the system size. Therefore, FN-QMC calculations still provide the most accurate values of ground-state properties of extended fermion systems.

Modification of the nodes of a many-fermion wave function to explicitly include correlations remains a formidable task. Slater determinants based on backflow (BF) coordinates present one possibility [7–10], and BF wave functions have been routinely used over the past years in QMC calculations of the electron gas [11–13] and liquid ^{3}He [14–18]. Generalization of the BF wave function to include three-body correlations was shown to be necessary to stabilize the unpolarized phase of liquid ^{3}He against spin polarization [19].

Here we propose new correlated trial wave functions based on iterative BF transformations and use them to study liquid ^{3}He in two dimensions. We show that this new class of trial wave functions systematically lowers the energy and its variance. Our results illustrate the possibility of extrapolating variational Monte Carlo (VMC) and FN diffusion Monte Carlo (DMC) calculations to zero variance to approach very closely the *exact* ground-state energy. Since their evaluation remains of similar complexity and scaling with increasing system size as the usual BF wave function, their use is not limited to small systems. We explicitly demonstrate the size consistency of our new trial wave functions and discuss the possibility of obtaining lower bounds to the ground-state energy.

II. ITERATED RENORMALIZATION OF WAVE FUNCTION

Let us start by considering the standard Slater-Jastrow-type trial wave function with BF:

$$\Psi_T^{(0)} = \det \phi_k(\mathbf{q}_i[\mathbf{R}]) e^{-U[\mathbf{R}]}. \tag{1}$$

Antisymmetry is ensured by the Slater determinant of single-particle orbitals, $\phi_k(\mathbf{r})$, $k = 1, \ldots, N$, where, instead of the bare coordinates $\mathbf{r}_i$, $i = 1, \ldots, N$, many-body BF coordinates, $\mathbf{q}_i$, are used as arguments. Both BF coordinates, $\mathbf{Q} = (\mathbf{q}_1, \ldots, \mathbf{q}_N)$, and the symmetric Jastrow potential, U, depend explicitly on all coordinates, $\mathbf{R} = (\mathbf{r}_1, \mathbf{r}_2, \ldots, \mathbf{r}_N)$, as indicated. In the standard form, $U = \sum_{i<j} u(r_{ij}) + \sum_i \mathbf{G}_i(\mathbf{R}) \cdot \mathbf{G}_i(\mathbf{R})$, with $\mathbf{G}_i = \sum_j (\mathbf{r}_i - \mathbf{r}_j)\xi(r_{ij})$, $\mathbf{q}_i = \mathbf{r}_i + \sum_j (\mathbf{r}_i - \mathbf{r}_j)\eta(r_{ij})$, and $r_{ij} = |\mathbf{r}_i - \mathbf{r}_j|$. The radial functions u, ξ, and η can be parametrized and optimized by minimization of the variational energy. Generalizations to include higher correlations into both BF and Jastrow potentials are possible [19] but are not considered here.

Once the BF and Jastrow potentials have been determined [20], different occupations of the orbitals inside the Slater determinant of Eq. (1) can be used to approximate also low-lying excited states of the systems, in close analogy to Landau's Fermi liquid description. As in the correlated basis functions approach [21,22], let us consider the effective Hamiltonian within these nonorthogonal basis states. For a Fermi liquid, we expect nondiagonal matrix elements of the effective Hamiltonian to be strongly suppressed compared to those of the bare plane-wave states. However, instead of diagonalizing the effective Hamiltonian, let us search again for a trial wave function to represent the ground state of the effective Hamiltonian. Assuming a smoothly varying effective interaction, we may again consider representing it as a BF wave function, $\Psi_T^{(1)}$. However, this time, the new BF coordinates, $\mathbf{q}_i^{(1)}$, and the new Jastrow potential, $U^{(1)}$, are built upon the old BF coordinates, $\mathbf{Q}^{(1)}[\mathbf{Q}^{(0)}]$, and $U^{(1)}[\mathbf{Q}^{(0)}]$ with $\mathbf{Q}^{(0)} \equiv \mathbf{Q}$. Thus

we are naturally led to an iterative renormalization procedure,

$$\Psi_T^{(\alpha)} \to \Psi_T^{(\alpha+1)} = \det \phi_k\left(\mathbf{q}_i^{(\alpha+1)}\right) e^{-U^{(\alpha+1)}}, \tag{2}$$

with a renormalized Jastrow potential

$$U^{(\alpha)} = \sum_{\beta\leqslant\alpha}\left[\sum_{i<j} u^{(\beta)}\left(q_{ij}^{(\beta-1)}\right) + \sum_i \mathbf{G}_i^{(\beta)}(\mathbf{Q}^{\beta-1})\cdot\mathbf{G}_i^{(\beta)}(\mathbf{Q}^{\beta-1})\right] \tag{3}$$

and renormalized BF coordinates

$$\begin{aligned}\mathbf{q}_i^{(\alpha)} &= \mathbf{r}_i + \sum_{\beta\leqslant\alpha}\mathbf{y}_i^{(\beta)},\\ \mathbf{y}_i^{(\alpha)}[\mathbf{Q}^{(\alpha-1)}] &= \sum_{j\neq i}\left(\mathbf{q}_i^{(\alpha-1)} - \mathbf{q}_j^{(\alpha-1)}\right)\eta^{(\alpha)}\left(q_{ij}^{(\alpha-1)}\right)\end{aligned} \tag{4}$$

[in Eqs. (3) and (4), $\mathbf{Q}^{(-1)}$ stands for $\mathbf{R}$]. At each iteration new potentials parametrizing the additional Jastrow and BF functions are introduced, and all the potentials $u^{(\beta)}$, $\xi^{(\beta)}$, and $\eta^{(\beta)}$, with $\beta \leqslant \alpha$, have to be optimized.

In the Appendix we show how the evaluation of the renormalized wave functions and their derivatives needed to calculate the local energy can be efficiently implemented with a number of operations proportional to N^3. Thus, the overall cost of calculation is not dramatically altered compared to that of the usual (zeroth-order) BF wave function. For a system of $N = 26$ particles we find that the CPU time to move all the particles and calculate the local energy with iterated BF of order 1 to 4 is a factor of 5, 9, 13, and 17 larger than that of the zeroth order, respectively; furthermore, for $N = 58$, fourth-order BF takes 12.5 times longer than for $N = 26$, close to the N^3 scaling. The corresponding figures for the efficiency of the calculation of the energy are even more favorable, because the variance is lower for improved wave functions.

III. TWO-DIMENSIONAL LIQUID ^{3}He AT FREEZING DENSITY

In order to illustrate the accuracy of the renormalization procedure to describe the ground-state wave function of highly correlated Fermi liquids, we perform calculations for the ground-state energy of liquid ^{3}He in two dimensions at a density $\rho = 0.060$ Å^{-2}, near freezing [4]. We compare VMC and FN-DMC energies to exact results obtained by the nominally exact transient estimate (TE) method of Ref. [3], for systems of $N = 26$ ($N = 29$) unpolarized (polarized) ^{3}He atoms interacting with the HFDHE2 potential [23]. Furthermore, we test the size consistency of our trial functions, comparing the gain in variational energy obtained by the renormalization procedure for the unpolarized system at two sizes, $N = 26$ and $N = 58$. The results are listed in Table I.

Every iteration introduces three new potentials (for BF, two-body, and three-body Jastrow function), each of which, generically indicated here as $f(r)$, is parametrized in the form

$$f(r) = \begin{cases}(r_C - r)^3\left[\sum_{n=1}^5 a_n r^{n-1} + a_6/r^{a_7}\right] & \text{if} \quad r < r_C,\\ 0 & \text{if} \quad r \geqslant r_C.\end{cases} \tag{5}$$

For the BF and three-body Jastrow potentials we set $r_C = 7$ Å and drop the McMillan term ($a_6 = 0$), while for the two-body Jastrow potential we choose a cutoff value r_C close to half the size of the simulation box. In Fig. 1 we show the optimized potentials $u^{(\alpha)}$, $\xi^{(\alpha)}$, and $\eta^{(\alpha)}$ of the $\Psi_T^{(4)}$ wave function for a system with $N = 26$ and $\zeta = 0$. The BF coordinate transformations across different iterations implicitly build up many-body correlations at all orders, so that eventually not all of the optimized potentials have an obvious physical interpretation: for instance, the pair distribution functions g of the bare coordinates and of the renormalized coordinates at subsequent iteration levels, shown in Fig. 2, feature increasingly wide correlation holes and high peaks for increasing level, despite

TABLE I. Ground-state energy per particle (in K) of liquid ^{3}He in two dimensions at $\rho = 0.060$ Å^{-2}, obtained with variational (E_T/N) and fixed-node diffusion Monte Carlo ($E_{\rm DMC}/N$) using different types of trial wave functions: the Slater-Jastrow wave function without backflow (PW) and with α-times-iterated backflow [BF$^{(\alpha)}$]. ζ is the spin polarization and N is the number of particles. Δ is the gain in variational Monte Carlo (VMC) energy per particle relative to the PW value, and σ^2 is the variance of the VMC total energy. TE indicates unbiased results calculated with the *transient estimate* method of Ref. [3]. VMC$_{\rm ext}$, DMC$_{\rm ext}$, and LB$_{\rm ext}$ are the extrapolations to zero variance of E_T/N, $E_{\rm DMC}/N$, and the lower bound $(E_T - \sqrt{\sigma^2})/N$, respectively. Statistical uncertainties on the last digit(s) are given in parentheses. All values are given for periodic boundary conditions (Γ point) without tail corrections [23].

	$N=26,\ \zeta=0$				$N=58,\ \zeta=0$				$N=29,\ \zeta=1$			
	E_T/N	σ^2/N	Δ	$E_{\rm DMC}/N$	E_T/N	σ^2/N	Δ	$E_{\rm DMC}/N$	E_T/N	σ^2/N	Δ	$E_{\rm DMC}/N$
PW	3.011(1)	28.29		2.419(2)	2.900(1)	28.07		2.373(2)	2.5831(6)	7.51		2.402(1)
BF$^{(0)}$	2.688(1)	13.05	0.323	2.353(2)	2.584(1)	13.34	0.316	2.283(2)	2.5133(5)	5.34	0.070	2.4005(6)
BF$^{(1)}$	2.471(1)	4.58	0.540	2.336(2)	2.356(2)	4.93	0.544		2.4383(3)	2.20	0.145	2.3918(5)
BF$^{(2)}$	2.4258(8)	2.86	0.585	2.3284(9)	2.313(2)	3.25	0.587		2.4193(3)	1.54	0.164	2.3877(4)
BF$^{(3)}$	2.4049(9)	2.47	0.606	2.3223(4)	2.297(2)	2.67	0.603		2.4136(2)	1.36	0.170	2.387(1)
BF$^{(4)}$	2.400(1)	2.29	0.611	2.323(1)	2.292(1)	2.49	0.608	2.232(1)	2.4109(7)	1.25	0.173	2.3869(5)
VMC$_{\rm ext}$		2.338(5)				2.217(2)				2.384(6)		
DMC$_{\rm ext}$		2.317(3)				2.216(3)				2.379(1)		
LB$_{\rm ext}$		2.275(14)				2.149(12)				2.390(26)		
TE		2.307(7)								2.375(3)		

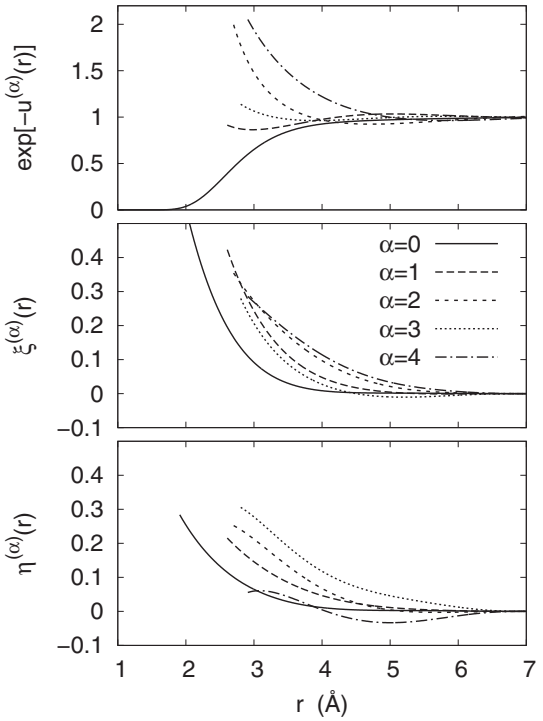

FIG. 1. Optimized potentials of the trial function $\Psi_T^{(4)}$ for $N = 26$, $\zeta = 0$. Lines are broken where the pair distribution functions of the relevant (quasi)coordinates become negligibly small, $g(r) \lesssim 10^{-3}$ (see Fig. 2).

the two-body potentials $u^{(\alpha)}$ turning from repulsive for $\alpha = 0$ to attractive for $\alpha = 4$. Note that all the g's feature the structure of simple liquids (albeit with increasingly classical character), which supports the heuristic derivation given in Sec. II: each iteration essentially renormalizes the Slater Jastrow wave function without qualitative changes.

With the choice of Eq. (5), the renormalization procedure requires 17 variational parameters per level, and the corresponding optimization procedure (carried out by correlated sampling [24] in this work) becomes rather demanding. Therefore we have tried two simpler iterative schemes, one in which no renormalized Jastrow is present and one in which only the new potentials added at the αth iteration

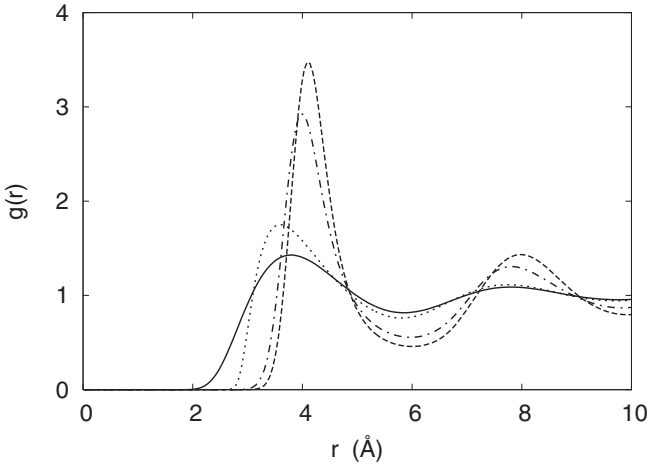

FIG. 2. Pair correlation functions calculated in a VMC simulation with the $BF^{(4)}$ trial function using the bare coordinates $\{\mathbf{r}_i\}$ (solid line) and the renormalized backflow coordinates $\{\mathbf{q}_i^{(0)}\}$, $\{\mathbf{q}_i^{(2)}\}$, and $\{\mathbf{q}_i^{(4)}\}$ (dotted, dash-dotted, and dashed lines, respectively). The statistical noise reaches its maximum value, ∼0.003, at the highest peak.

are optimized, leaving the others unchanged from previous iterations. However, these simpler options lead to higher values in energy, for both the VMC and the DMC. We have also considered an improved wave function with different BF potentials for parallel and antiparallel spins. The gain in energy is ∼10 mK in the VMC but hardly visible in the DMC ($\lesssim$1 mK) beyond the second BF iteration. Finally, we have tested the accuracy of using potentials optimized for $N = 26$ to perform simulations with $N = 58$ particles: at the fourth BF iteration, the DMC energy is higher by a non-negligible amount, 5 ± 2 mK. All these results are listed in Table II.

IV. ZERO-VARIANCE EXTRAPOLATION AND LOWER BOUNDS

Our VMC and FN-DMC results for the energy expectation values $E_X = \langle \Psi_X | H | \Psi_X \rangle$ of the different (normalized) wave functions provide strict upper bounds for the true ground-state energy, $E_0 \leqslant E_X$, where the subscript X stands for T or DMC as appropriate and Ψ_{DMC} is the FN ground state. Within

TABLE II. Some of the energies in Table I compared to the corresponding values obtained with downgraded or upgraded wave functions. Entries 0, energies from Table I; entries I, downgraded wave functions with omitted Jastrow factors of the quasicoordinates; entries II, downgraded wave functions with Jastrow and backflow potentials from previous iterations not repotimized; entries III, upgraded wave functions with different like-spin and unlike-spin backflow potentials; entries IV, downgraded wave functions for $N = 58$ with Jastrow and backflow potentials optimized for $N = 26$.

	$N = 26, \zeta = 0$								$N = 58, \zeta = 0$			
	E_T/N				E_{DMC}/N				E_T/N		E_{DMC}/N	
	0	I	II	III	0	I	II	III	0	IV	0	IV
PW									2.900(1)	2.909(2)		
$BF^{(0)}$									2.584(1)	2.592(2)	2.289(2)	2.288(1)
$BF^{(1)}$	2.471(1)	2.599(2)	2.515(1)	2.461(1)	2.336(2)	2.337(2)	2.337(2)					
$BF^{(2)}$	2.4258(8)	2.585(2)	2.480(1)	2.413(1)	2.3284(9)	2.335(2)	2.332(1)	2.3256(9)				
$BF^{(3)}$	2.4049(9)	2.584(2)	2.472(1)	2.398(1)	2.3223(4)	2.335(2)	2.326(1)	2.3215(4)				
$BF^{(4)}$	2.400(1)	2.580(2)	2.470(1)	2.390(2)	2.323(1)	2.331(1)	2.325(3)	2.324(1)	2.292(1)	2.298(2)	2.232(1)	2.237(1)

the VMC, we also have access to the variance of the energy in the trial state, $\sigma^2 = \langle \Psi_T | (H - E_T)^2 | \Psi_T \rangle$. As the variance approaches 0 for any exact eigenstate, its value for a given trial wave function can be used to quantify the distance to the closest eigenfunction. Under the assumption that the trial energy is closer to the ground-state energy than to any of the other eigenstates, the inequality $\sigma^2 \geqslant (E_0 - E_T)^2$ leads to a lower bound for the ground-state energy [25–27]:

$$E_0 \geqslant E_T - \sqrt{\sigma^2}. \tag{6}$$

Note that the above assumption for the validity of this bound implies that the trial energy per particle approaches the exact ground-state energy per particle for extended systems in the thermodynamic limit, which would make the bound of rather limited interest. However, in the following, we show that the lower-bound expression remains valid under much weaker assumptions and applicable for finite systems of commonly used sizes. Further, we use the information on the variance obtained by VMC to extrapolate trial energies to the exact ground-state energy.

Let us first analyze in more detail how the trial wave function approaches the ground-state wave function. Expanding our trial wave function in the exact eigenstates, $|E_j\rangle$, of energy E_j, we have $|\Psi_T\rangle = \sum_j c_j |E_j\rangle$, where c_j are the expansion coefficients, with $\sum_j |c_j|^2 = 1$ assuming normalized states. We can now write

$$E_T = E_0 + \Delta_T C_T, \tag{7}$$

with $C_T = \sum_{j\neq 0}^{M} |c_j|^2$ and $\Delta_T \equiv \sum_i (E_i - E_0) c_i^2 / C_T \geqslant \Delta$, where $\Delta \equiv E_1 - E_0$ denotes the energy gap between the ground and the first excited state of the system. Similarly, we obtain for the variance

$$\sigma^2 = \overline{\Delta^2}_T C_T - (\Delta_T C_T)^2, \tag{8}$$

where $\overline{\Delta^2}_T \equiv \sum_i (E_i - E_0)^2 c_i^2 / C_T \geqslant \Delta_T^2$.

Using Eqs. (7) and (8) we have

$$E_T - \sqrt{\sigma^2} = E_0 - \Delta_T C_T \left[\sqrt{\frac{\overline{\Delta^2}_T}{\Delta_T^2 C_T} - 1} - 1 \right], \tag{9}$$

and we see that the expression for the lower bound, Eq. (6), remains valid for $C_T \leqslant \overline{\Delta^2}_T / 2\Delta_T^2$ or $E_T - E_0 \leqslant \overline{\Delta^2}_T / 2\Delta_T$. Note that this condition is less stringent than the assumption that E_T is closer to the ground-state energy than to any of the other eigenstates used previously.

To go further, let us assume that the trial wave function has a significant overlap only with the ground-state wave function, whereas the components of excited states, c_i with $i > 0$, are broadly distributed. We expect this assumption to be reasonably satisfied for extended systems, where the excited states approach a continuum in the thermodynamic limit. Improving the wave function via our iterative renormalization, the excited-state contributions decrease almost uniformly, such that $C_T \to 0$ whereas Δ_T and $\overline{\Delta^2}_T$ remain roughly constant. In this case we can neglect terms of order C_T^2 in Eq. (8), insert it in Eq. (7), and obtain

$$E_T = E_0 + A\,\sigma^2 \quad \text{for} \quad \sigma^2 \to 0, \tag{10}$$

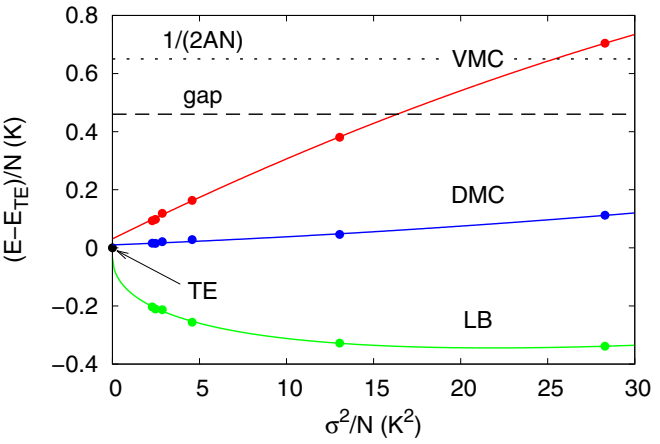

FIG. 3. (Color online) VMC and DMC energies per particle of $N = 26$ unpolarized ^{3}He atoms in two dimensions as a function of the variance σ^2/N. Each point corresponds to a different trial function [PW and $\mathrm{BF}^{(\alpha)}$ with $\alpha = 0$ to 4, from higher to lower variance]. The TE energy has been subtracted. Their dependence is nearly linear, and their extrapolations to zero variance, the entries $\mathrm{VMC}_{\mathrm{ext}}$ and $\mathrm{DMC}_{\mathrm{ext}}$ in Table I, are very close to the exact result. We further show the energy lower bound $(E_T - \sqrt{\sigma^2})/N$, whose extrapolation to zero variance, the entry $\mathrm{LB}_{\mathrm{ext}}$ in Table I, is also very close to the exact result. The dashed line is a rough estimate of the first excited state (the difference between the two slowest exponential decay constants in the fermionic signal of the TE procedure [3]). It shows that the conditions for the validity of the energy lower bound (see text) are met by the iterated backflow trial functions. The dotted line is the alternate estimate $1/(2AN)$ of Eq. (11) for the validity of the lower bound.

with $A = \Delta_T / \overline{\Delta^2}_T$. Therefore, with good enough trial functions, we expect that a (nearly) linear extrapolation of the variational energy to zero variance closely approaches the exact ground-state energy, with the coefficient of the linear term providing a numerical estimate of the validity of the lower bound of Eq. (6); i.e.,

$$E_T - E_0 \leqslant 1/(2A). \tag{11}$$

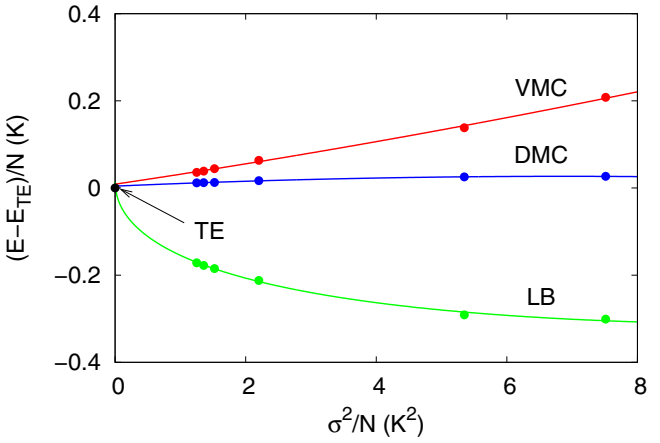

FIG. 4. (Color online) Same as Fig. 3, for $N = 29$ spin-polarized ^{3}He atoms. Both the estimate of the first excited state, ~0.6 K, and the value of $1/(2AN)$, 0.772 K, are off scale.

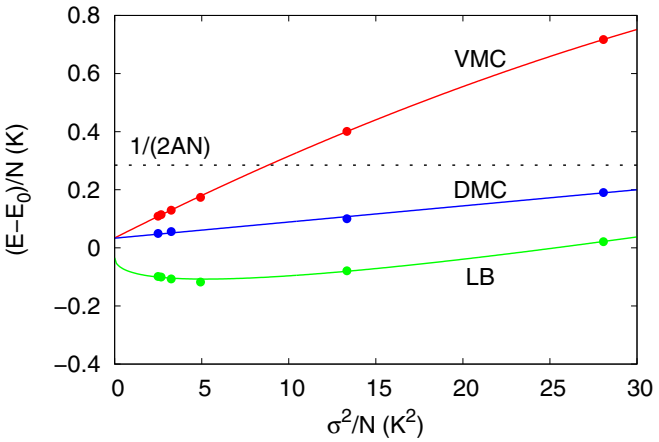

FIG. 5. (Color online) Same as Fig. 3, for $N = 58$ unpolarized ^{3}He atoms. Due to the lack of TE results, we take a reference energy E_0/N halfway between $\mathrm{VMC_{ext}}$ and $\mathrm{LB_{ext}}$. Also, we do not have an estimate of the first excited state. Comparison of the dotted line here with that in Fig. 3 shows that the range of $E_T - E_0$ where the lower bound is expected to be valid shrinks as $1/N$.

The lower bound, in turn, can be made stricter by extrapolation to zero variance of $E_T - \sqrt{\sigma^2}$ with a leading square-root term. These variance extrapolations are shown in Figs 3, 4, and 5 and listed in Table I.

All of the above extrapolations are valid for $C_T \to 0$. Using a general estimate for the overlap of the trial wave function with the ground state [28], $C_T \equiv 1 - c_0^2 \geqslant 1 - \exp[-(E_T - E_0)^2/2\sigma^2] \approx 1 - \exp[-A^2\sigma^2]$, we can *a posteriori* check the consistency of the energy-versus-variance extrapolation, leading to the condition that $A^2\sigma^2$ be significantly smaller than 1.

Finally, one would like to use variance extrapolation with the FN energies to obtain even better results. However, within the DMC, the variance $\langle\Psi_{\mathrm{DMC}}|(H - E_{\mathrm{DMC}})^2|\Psi_{\mathrm{DMC}}\rangle$ is 0 inside any nodal pocket [29] and can no longer be used as a measure of the quality of the wave function. The most natural assumption is then to postulate that the variance σ^2 calculated in the VMC is a good measure of the quality of the wave function in the DMC as well. This allows us to use the same extrapolation for DMC energies as in the case of the VMC, as shown in Figs. 3–5, but without obtaining a lower bound. The DMC energy extrapolated to zero variance, listed in Table I, happens to differ from the TE value by just the combined error bar, 10 mK for $\zeta = 0$ and 4 mK for $\zeta = 1$.

V. CONCLUSIONS

In this paper we have introduced new, highly correlated wave functions for accurate descriptions of normal Fermi liquids based on generalized BF coordinates which are iteratively improved. For unpolarized liquid ^{3}He at freezing density, the energy gain of these wave functions at the fourth iteration compared to the usual BF trial wave function (0 iterations) is about 290 mK within the VMC and 50 mK (30 mK) for the FN-DMC with $N = 58$ ($N = 26$) atoms. More important, we have shown that the true ground-state energy can be obtained by variance extrapolation with intrinsic *a posteriori* checks of the consistency and validity of the extrapolation. For a small number of atoms, $N \sim 26$, we have shown that the obtained results are in agreement with unbiased calculations using TEs, but variance extrapolation can also be used to quantify the FN error of larger systems. For systems with $N = 58$ atoms, the FN error of our best wave function is around 15 mK.

Thus, apart from significant VMC and FN-DMC energy gains, the iterative BF renormalization procedure also leads to a general strategy to quantify the FN error of the calculations. In combination with finite-size extrapolations based on the analytical informations contained in the trial wave function [30,31], the methods presented in the paper provide an important step towards the control of the accuracy of QMC calculations suffering from a Fermion sign problem.

ACKNOWLEDGMENTS

M.H. thanks Bernard Bernu, David Ceperley, and Lubos Mitas for discussions. Computer time at CNRS-IDRIS is acknowledged (Project No. i2014051801).

APPENDIX: COMPUTATIONAL DETAILS

Let us suppose that q_i^α are BF coordinates $i = 1, \ldots, N$ and $\alpha = 1, \ldots, d$, where d is the spatial dimension, and we have already computed the following partial derivatives:

$$Q_{ij}^{\alpha\beta} \equiv \nabla_i^\alpha q_j^\beta, \tag{A1}$$

$$\widetilde{Q}_j^\beta \equiv \Delta q_j^\beta \equiv \sum_{i\alpha} \nabla_i^\alpha \nabla_i^\alpha q_j^\beta. \tag{A2}$$

We further need

$$\overline{Q}_{lm}^{\beta\gamma} = \sum_{i\alpha} Q_{il}^{\alpha\beta} Q_{im}^{\alpha\gamma}, \tag{A3}$$

which is already needed for computation of the local energy of the Slater determinant using orbitals based on the above BF coordinates [11], which we shortly review.

1. Backflow determinant

The gradient and the Laplacian of a determinant, $D = \det \varphi_{ki}$, with BF coordinates in the orbitals, $\varphi_{ki} \equiv \varphi_k(\mathbf{q}_i)$, can be calculated as

$$\nabla_i^\alpha \log D = \sum_{j\beta} F_{jj}^\beta Q_{ij}^{\alpha\beta}, \tag{A4}$$

$$\Delta \log D = \sum_{i\alpha} F_{ii}^\alpha \widetilde{Q}_i^\alpha + \sum_{i\alpha\beta} \left[\sum_m V_{im} \varphi_{mi}^{\alpha\beta} \right] \overline{Q}_{ii}^{\alpha\beta} - \sum_{ij\alpha\beta} F_{ij}^\alpha F_{ji}^\beta \overline{Q}_{ji}^{\alpha\beta}, \tag{A5}$$

where

$$\varphi_{ki}^\alpha \equiv \frac{\partial \varphi_{ki}}{\partial q_i^\alpha}, \quad \varphi_{ki}^{\alpha\beta} \equiv \frac{\partial^2 \varphi_{ki}}{\partial q_i^\alpha \partial q_i^\beta}, \quad F_{ij}^\alpha = \sum_k V_{ik} \varphi_{kj}^\alpha \tag{A6}$$

and V_{ik} is the inverse of the BF matrix,

$$V_{ik} = \frac{1}{D}\frac{\partial D}{\partial \varphi_{ki}}, \quad \sum_k V_{ik}\varphi_{kj} = \delta_{ij}. \tag{A7}$$

The computational complexity is of order N^3 for the inversion of the orbital matrix, V_{ik}, as well as for the computation of the matrices F_{ij}^{α} and $\overline{Q}_{ij}^{\alpha\beta}$.

Note that this part of the calculations does not depend on the specific form of the BF coordinates. The computation of the gradient and Laplacian of the local energy based on Eq. (A4) and Eq. (A5) depends only on the actual values of the orbital matrix, φ_{ki}, and its partial derivatives, Eq. (A6), and on the gradient and Laplacian of the BF coordinates, Eqs. (A1) and (A2). Therefore, Eqs. (A4) and (A5) can still be used to calculate the local energy of determinants containing iterated BF coordinates, as long as their derivatives are provided in the form of Eqs. (A1), (A2), and (A3).

2. Iterated Jastrow correlations

We can now build a Jastrow factor based on the distances between two quasiparticles,

$$U = \sum_{l<m} u(q_{lm}), \tag{A8}$$

where u denotes the function and $u'(u'')$ its first (second) derivative. The gradient of the Jastrow factor can then be calculated by the chain rule,

$$\nabla_i^{\alpha} U = \sum_{l\beta} V_l^{\beta} Q_{il}^{\alpha\beta}, \quad V_l^{\beta} = \sum_{m\neq l} \frac{u'(q_{lm})}{q_{lm}} q_{lm}^{\beta}, \tag{A9}$$

and

$$\Delta U = \sum_{l\beta} V_l^{\beta}\widetilde{Q}_l^{\beta} + \sum_{l\neq m}\sum_{\beta\gamma} W_{lm}^{\beta\gamma}\left[\overline{Q}_{ll}^{\beta\gamma} - \overline{Q}_{lm}^{\beta\gamma}\right], \tag{A10}$$

with

$$W_{lm}^{\beta\gamma} = \left(u''(q_{lm}) - \frac{u'(q_{lm})}{q_{lm}}\right)\frac{q_{lm}^{\beta}q_{lm}^{\gamma}}{q_{lm}^2} + \delta_{\beta\gamma}\frac{u'(q_{lm})}{q_{lm}}. \tag{A11}$$

We see that the overall cost of the quasiparticle Jastrow factor and its derivatives needed for the local energy is of the order of N^3, needed to build the matrix $\overline{Q}_{lm}^{\beta\gamma}$, Eq. (A3). Since this matrix is already needed in the calculation of the usual BF wave function [11], the iterated Jastrow does not lead to a significant slowdown compared to the usual BF.

3. Iterated BF coordinates

We now construct new BF coordinates,

$$y_i^{\alpha} = \sum_{j\neq i} q_{ij}^{\alpha}\eta(q_{ij}), \tag{A12}$$

where η is the corresponding potential. In order to calculate the local energy for BF orbitals in the Slater determinant based on y_i^{α}, we need the following derivatives:

$$Y_{ij}^{\alpha\beta} \equiv \nabla_i^{\alpha} y_j^{\beta}, \quad \widetilde{Y}_i^{\alpha} \equiv \Delta y_i^{\alpha}. \tag{A13}$$

In order to calculate them, we use the chain rule, based on the partial derivatives

$$\frac{\partial y_j^{\beta}}{\partial q_i^{\alpha}} = \delta_{ij}\sum_n \dot{y}_{in}^{\alpha\beta} - \dot{y}_{ij}^{\alpha\beta},$$

$$\frac{\partial^2 y_k^{\gamma}}{\partial q_i^{\alpha}\partial q_j^{\beta}} = \delta_{ijk}\sum_n \ddot{y}_{kn}^{\alpha\beta\gamma} - \delta_{jk}\ddot{y}_{ki}^{\alpha\beta\gamma} - \delta_{ij}\ddot{y}_{jk}^{\alpha\beta\gamma} - \delta_{ik}\ddot{y}_{kj}^{\alpha\beta\gamma},$$

where

$$\dot{y}_{ij}^{\alpha\beta} = \frac{\eta'(q_{ij})}{q_{ij}} q_{ij}^{\alpha} q_{ij}^{\beta} + \eta(q_{ij})\delta_{\alpha\beta},$$

$$\ddot{y}_{ij}^{\alpha\beta\gamma} = \left[\eta''(q_{ij} - \frac{\eta'(q_{ij})}{q_{ij}}\right]\frac{q_{ij}^{\alpha}q_{ij}^{\beta}q_{ij}^{\gamma}}{q_{ij}^2} + \frac{\eta'(q_{ij})}{q_{ij}}\left[q_{ij}^{\alpha}\delta_{\beta\gamma} + q_{ij}^{\beta}\delta_{\alpha\gamma} + q_{ij}^{\gamma}\delta_{\alpha\beta}\right],$$

and we have used that $\dot{y}_{ii}^{\alpha\beta} = \ddot{y}_{ii}^{\alpha\beta\gamma} = 0$.

The final derivatives needed, Eq. (A13), can then be written as

$$Y_{ij}^{\alpha\beta} = \sum_{n\gamma} \dot{y}_{jn}^{\gamma\beta}\left[Q_{ij}^{\alpha\gamma} - Q_{in}^{\alpha\gamma}\right],$$

$$\widetilde{Y}_i^{\alpha} = \sum_{n\beta} \dot{y}_{in}^{\alpha\beta}\left[\widetilde{Q}_i^{\beta} - \widetilde{Q}_n^{\beta}\right] + \sum_{n\alpha\beta} \ddot{y}_{in}^{\alpha\beta\gamma}\left[\overline{Q}_{ii}^{\beta\gamma} + \overline{Q}_{nn}^{\beta\gamma} - 2\overline{Q}_{in}^{\beta\gamma}\right]. \tag{A14}$$

Again, these operations can be done in the order of N^3 computations.

4. Iterated *n*-body correlations

Above we have explicitly shown how to calculate the gradient and Laplacian of a scalar two-body Jastrow potential and of quasiparticle coordinates constructed from BF coordinates. The structure of our three-body correlation in Eq. (3) is actually a scalar product between two vectors with identical structure as the BF coordinates. The gradient and Laplacian of the three-body term can therefore be calculated from those of the vectors using the chain rule. Generalizations to build iterated many-body Jastrow and BF coordinates based on quasiparticle tensors [19] are straightforward and do not increase the complexity of the calculation.

5. Higher order iterations

At the zeroth order of iteration, the BF coordinates, $\mathbf{q}_i$, are symmetric functions of the bare coordinates. Higher order iterations of the BF are built from symmetric expressions based on the previous BF coordinates, such that the overall wave function remains antisymmetric. Above, we have explicitly shown how to calculate the gradient and the Laplacian of the quasiparticle coordinates of the first BF iteration, $\mathbf{q}_i^{(1)} \equiv \mathbf{q}_i + \mathbf{y}_i$, without increasing the overall complexity of the calculation. These are the only additional information needed to calculate the local energy of the first iterated BF determinant, and from the structure it is clear that this procedure can be iterated to higher order without increasing the complexity of the calculations.

[1] P. J. Reynolds, D. M. Ceperley, B. J. Alder, and W. A. Lester, J. Chem. Phys. **77**, 5593 (1982).

[2] D. M. Ceperley and B. J. Alder, J. Chem. Phys. **81**, 5833 (1984).

[3] G. Carleo, S. Moroni, F. Becca, and S. Baroni, Phys. Rev. B **83**, 060411(R) (2011).

[4] M. Nava, A. Motta, D. E. Galli, E. Vitali, and S. Moroni, Phys. Rev. B **85**, 184401 (2012).

[5] J. J. Shepherd, G. Booth, A. Grüneis, and A. Alavi, Phys. Rev. B **85**, 081103(R) (2012).

[6] F. Pederiva, S. A. Vitiello, K. Gernoth, S. Fantoni, and L. Reatto, Phys. Rev. B **53**, 15129 (1996); F. Calcavecchia, F. Pederiva, M. H. Kalos, and T. D. Kühne, Phys. Rev. E **90**, 053304 (2014).

[7] V. R. Pandharipande and N. Itoh, Phys. Rev. A **8**, 2564 (1973).

[8] K. E. Schmidt and V. R. Pandharipande, Phys. Rev. B **19**, 2504 (1979).

[9] E. Manousakis, S. Fantoni, V. R. Pandharipande, and Q. N. Usmani, Phys. Rev. B **28**, 3770 (1983).

[10] S. A. Vitiello, K. E. Schmidt, and S. Fantoni, Phys. Rev. B **55**, 5647 (1997).

[11] Y. Kwon, D. M. Ceperley, and R. M. Martin, Phys. Rev. B **48**, 12037 (1993).

[12] Y. Kwon, D. M. Ceperley, and R. M. Martin, Phys. Rev. B **58**, 6800 (1998).

[13] M. Holzmann, D. M. Ceperley, C. Pierleoni, and K. Esler, Phys. Rev. E **68**, 046707 (2003).

[14] K. E. Schmidt, M. A. Lee, M. H. Kalos, and G. V. Chester, Phys. Rev. Lett. **47**, 807 (1981).

[15] R. M. Panoff and J. Carlson, Phys. Rev. Lett. **62**, 1130 (1989).

[16] J. Casulleras and J. Boronat, Phys. Rev. Lett. **84**, 3121 (2000).

[17] S. Moroni, S. Fantoni, and G. Senatore, Phys. Rev. B **52**, 13547 (1995).

[18] F. H. Zong, D. M. Ceperley, S. Moroni, and S. Fantoni, Mol. Phys. **101**, 1705 (2003).

[19] M. Holzmann, B. Bernu, and D. M. Ceperley, Phys. Rev. B **74**, 104510 (2006).

[20] W. L. McMillan, Phys. Rev. **138**, A442 (1965).

[21] E. Feenberg, *Theory of Quantum Fluids* (Academic Press, New York, 1969).

[22] E. Krotscheck, in *Introduction to Modern Methods of Quantum Many-Body Theory and Their Applications*, edited by A. Fabrocini, S. Fantoni, and E. Krotscheck (World Scientific, Singapore, 2002).

[23] R. A. Aziz, V. P. S. Nain, J. S. Carley, W. L. Taylor, and G. T. McConville, J. Chem. Phys **70**, 4330 (1979). The potential is made to vanish at half the size of the simulation box by a rigid shift.

[24] D. M. Ceperley and M. H. Kalos, in *Monte Carlo Methods in Statistical Physics*, edited by K. Binder (Springer-Verlag, Berlin, 1979).

[25] G. Temple, Proc. Roy. Soc. Ser. A **119**, 276 (1928).

[26] D. H. Weinstein, Proc. Natl. Acad. Sci. USA **20**, 529 (1934).

[27] S. Goedecker and K. Maschke, Phys. Rev. B **44**, 10365 (1991).

[28] C. Mora and X. Waintal, Phys. Rev. Lett. **99**, 030403 (2007).

[29] Unless the nodes are exact, the FN-DMC wave function will have a discontinuous derivative at the nodal surface. Nevertheless, one can show that the energy expectation value of an FN-DMC wave function still provides an upper bound to the true ground-state wave function having continuous derivatives everywhere.

[30] S. Chiesa, D. M. Ceperley, R. M. Martin, and M. Holzmann, Phys. Rev. Lett. **97**, 076404 (2006).

[31] M. Holzmann, B. Bernu, V. Olevano, R. M. Martin, and D. M. Ceperley, Phys. Rev. B **79**, 041308(R) (2009); M. Holzmann, B. Bernu, C. Pierleoni, J. McMinis, D. M. Ceperley, V. Olevano, and L. Delle Site, Phys. Rev. Lett. **107**, 110402 (2011).